detritus | Multidisciplinary Journal for Circular Economy and Sustainable Management of Residues

CISA

APPLICATION OF A GAS-SOLID FLUIDISED BED SEPARATOR FOR ALUMINIUM-COPPER SCRAP RECYCLING

József Faitli [1], Ádám Rácz [1,*], Márton Vitányi [2] and Sándor Nagy [1]

[1] *Institute of Raw Materials Preparation and Environmental Technologies, University of Miskolc, Hungary*
[2] *Inter-metal Ltd., Budapest, Hungary*

Article Info:
Received:
20 March 2023
Revised:
16 June 2023
Accepted:
19 June 2023
Available online:
21 July 2023

Keywords:
Fluidised bed
Aero-suspension
Dense media separator
Aluminium and copper scrap
Bingham plastics
Powder rheology

ABSTRACT
The EU's circular economy concept necessitates the recycling of material streams used once or multiple times into the production–consumption cycle again and again. The commonly known problem – that the number of recycling cycles of plastics is limited – drives the economy towards metal usage again, because metal recycling cycles are limitless. Therefore, the efficient and economic separation of mixed aluminium and copper scraps in the 30–100 mm particle size range is an important issue for our society. In this study fundamental and applied research was carried out for the application of a gas-solid fluidised bed separator for aluminium-copper scrap recycling. A laboratory scale aero-suspension dense media separator was developed. Fundamental fluidisation experiments were carried out with this device and a powder rheometer. Afterwards pilot-scale and later industrial-scale separators were designed and built. The results indicate that the well-known Ergun fluidisation model can be the basis of a new process engineering design method for sizing dry fluidised bed separators.

1. INTRODUCTION

Among humanity's greatest challenges today is the provision of material and energy for civilised life. Even though the collection and recycling of scrap metals is only a very small part of the whole, if we do it in an energy-efficient way (Hou et al., 2022; Zhumadillayeva et al., 2020), we contribute to the goal of securing material for mankind. This is the research gap this paper addresses. The fluidised bed aero-suspension dense media separator is a well-known type of equipment (e.g., Anjaneyulu & Khakbar, 1995; Basu, 2006; Beeckmans & Minh, 1977; Gibilaro, 2001; Sahu et al., 2009; Fan and Zhou, 2021), however its design is still based on experiment, process engineering design methods need to be further improved.

Based on its operating principle, there is a solid-gas fluidised bed made by blown-in air from the bottom into the bulk granular separation medium. The mixture density of the fluidised solid-gas dense media can be controlled by the quantity of the air blown in. The heavier particles of the feed will sink, and lighter particles will float. Compared to wet dense media separation, there is no need for any liquid, and therefore no need for the clarification for the separated products or a water handling system. The dry fluidised bed method of separation needs to be explored because it produces low pressure drop and high efficiency (Anam & Ikhwan, 2020) and that helps with fulfilling the targeted aim of waste-to-material recycling for the circular economy. Therefore, dry dense media separators are widely applied in the industry. The first application of fluidisation was invented by Brötz in 1900 (Ghosh, 2013). Brötz applied a counter-current water flow to loosen a sand water filtration bed. Dry dense media separation is widely applied in the pharmaceutical industry (Dévay, 2013) and in waste management (Everett & Peirce, 1990). A gas-solid fluidised bed separator was applied on a laboratory scale for shredded municipal bulky solid waste separation (Sekito et al., 2006). The work of Sekito et al. (2006) was later further improved by Yoshida et al. (2010), when the chlorine content of processed plastic part of municipal solid wastes was significantly decreased by a fluidised bed dry separator. Separation of harmful impurities from refuse derived fuels (RDF) was carried out in a solid-gas fluidised bed (Krüger et al., 2014). There are other applications of dry fluidised bed separation technology for waste processing; Oshitani et al. (2003) used this technology for recycling automotive shredder residue materials.

There are several scientific and practical challenges to be solved for the development of a separation machine. The most important might be how to establish homogeneous solid-gas distribution in the fluidised bed. There are several unwanted phenomena that might occur during insufficient bed operation, such as bubbling, slugging, channelling and

* Corresponding author:
Ádám Rácz
email: adam.racz@uni-miskolc.hu

https://doi.org/10.31025/2611-4135/2023.18303

agitation, and turbulent fluidisation (Ghosh, 2013). Figure 1 shows the typical pressure loss of fluidised solid-gas beds as a function of the air velocity (Dévay, 2013; Thanh & Duc, 2020).

When the flow rate of air blowing is increased from 0 up point A the solids are still packed in the bed and the pressure loss increases linearly with air velocity because of the laminar flow between the particles (Dévay, 2013). Between points A and B, the velocity increases exponentially and from point B the solid particles start to levitate. Between points B and C they may have better orientation and that decreases the resistance; therefore, the pressure loss also decreases a little. From points B to E good fluidisation can be established. In this desirable zone the particles typically do not contact, they are levitating in the air stream, and the pressure loss does not depend on the fluid velocity, nor does it depend much on the solids concentration either in this zone. From point E, the transport of the particles starts, which is another process, namely pneumatic transport. This is clearly avoidable in fluidised bed technologies. Figure 1 is extremely important for the process engineering point of view. The air flow rate range between points D and E is small; it is a practical challenge to establish stable conditions here. The density of the fluidised solid-gas bed depends on the air flow rate in zone D-E and this range is limited. The density of the fluidised solid-gas bed is crucial for the separation because this is the cut density. The density of the applied solids as separation medium basically determines the mixture density. However, theoretically it is possible to set a different fluidised solid-gas bed density and therefore a different cut density by changing the air flow rate. According to Zhou et al. (2019) the bed density in the aero-suspension dense media separator can be determined theoretically for a given fluidisation air velocity using the two-phase theory, but empirical validation is necessary. Li et al. (2017) applied CFD techniques for fluidised-bed separator optimisation by using the composite force field or flow field to enhance the recovery of coarse particles and expand its application in the coarse coal slime separation and metal beneficiation. Zhao & Wei (2000) measured the rheological properties of fluidised aero suspensions with a settling body measurement device. If the solid-gas two-phase system is fluidised the mixture behaves like a one-phase fluid, and the rheological properties of this mixture can be interpreted and measured. However, if the fine solids are not fluidised, they behave totally differently; the phenomenon of powder flow happens in this case. According to Zhao & Wei (2000), fluidised aero suspensions are typically Bingham plastic fluids with two rheological features; namely, their viscous flow can be characterised by the yield stress and the plastic viscosity.

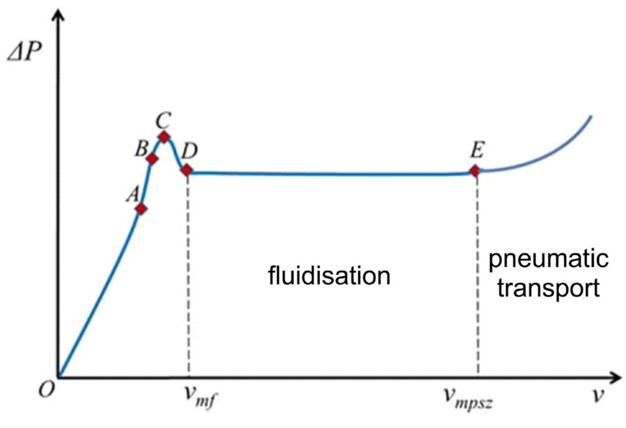

FIGURE 1: The pressure loss of fluidised solid-gas beds as function of the air velocity (Dévay, 2013).

Thanh & Duc (2020) summarised their theoretical and empirical results on dry fluidisation applied for the drying of refined salt. They comprehensively summarised the different theoretical models for the determination of the minimum fluidisation velocity in the literature. This is not repeated here (the equations of Kozeny-Carman, Wen-Yu, Beayens-Geldart, Goroshko, Goroshko-Todes, Leva and Kunii-Levenspiel are not); only the equations given afterwards are reported. The first equations and model of the field were published by Ergun in 1952. According to Ergun (1952), at the point of the "minimum particulate fluidisation state" (point D in Fig. 1) the air stream must have sufficient pressure and velocity to pass through the static bed of the dense fluidisation medium. The dense fluidisation medium can be characterised by the mean particle size (d_p), mean shape factor (F), mean particle density (r_p) and the void fraction (porosity) of the solids in the bed (e_{mf}). The applied shape factor here is the so-called surface proportional one. The volume of a non-spherical particle has to be determined first, and then the volume equivalent particle diameter can be calculated. The surface proportional shape factor is the ratio between the surface of the original particle and the surface of its volume equivalent sphere. Therefore, F=1 of a sphere because the specific surface of a sphere is the smallest. Physical properties (density r_f and absolute viscosity m_f) of air of the given temperature are known. The relationship between the air pressure (Dp) and minimum fluidisation velocity (V_{mf}) for any particle shape is given by Eq. 1.

$$\frac{\Delta p}{H_{mf}} = 150 \cdot \frac{(1-\varepsilon_{mf})^2}{\varepsilon_{mf}^3} \cdot \frac{\mu_f \cdot V_{mf}}{(\Phi \cdot d_m)^2} + 1.75 \cdot \frac{(1-\varepsilon_{mf})}{\varepsilon_{mf}^3} \cdot \frac{\rho_f V_{mf}^2}{\Phi \cdot d_m} \quad (1)$$

The pressure of the air stream at this minimum fluidisation point must be large enough to overcome the weight of the particles of the separation medium in the bed (Eq. 2).

$$\Delta p = \frac{m}{\rho_p \cdot A} \cdot (\rho_p - \rho_f) \cdot g \quad (2)$$

where A is the effective (used) cross section of the separator and m is the mass of the particles of the separation medium. Previously it was pointed out by Zhao and Wei (2000) that a flowing aero-suspension can be treated as a Bingham plastic behaviour fluid (equivalent liquid), but here at point D, the aero-suspension itself is quiescent. According to the model of Ergun (1952), we can talk about an air flow in the pores of the loosened particles of the separation medium with velocity v_{mf}, therefore a Reynolds number (Re_{mf}) can be defined using the physical properties of air and the $\Phi \cdot d_p$ term as the size parameter (Eq. 3).

$$Re_{mf} = \frac{\rho_f \cdot V_{mf} \cdot \Phi \cdot d_p}{\mu_f} \quad (3)$$

The gas-solid fluidised bed separator is an upgrading unit, because separation happens at a quality, namely at the density (Drzymala, 2007; Pillay et al., 2022). In this form this unit represents a two- product separation process. An upgrading separation process can be characterised by the yield, content, and recovery or loss values (Drzymala, 2007). Mass yield of product A (γ_A) equals the mass flow rate of product A over the mass flow rate of the feed. The component content of component 1 in the feed is λ_1 and in product A is α_1. By this data the component recovery of component 1 into product A is $\varepsilon=\gamma_A \cdot \lambda_1/\alpha_1$. The component loss can be calculated similarly, representing the unsuccessful separation of component 1 getting into product B.

To address the above-mentioned challenges, laboratory-scale test equipment has been developed. Our research team has carried out fundamental examinations of different air inlet systems to determine how to avoid phenomena that disturb stable fluidisation flow. The specific air flow rate and pressure - needed for a given height and material solid-gas fluidised bed - were measured. The air flow rate versus bed resultant density functions and the settling velocity of given scrap particles in solid-gas fluidised beds of given density were also measured. Based on the lab-scale examination a pilot-scale separator was designed and built. Fundamental research with the pilot scale machine was carried out and after that the industrial size separator was designed and built. Fundamental applied research with the industrial scale machine was carried out with aluminium–copper scraps.

2. MATERIALS AND METHODS

The research work described in the article was largely carried out with equipment created by the authors; this section presents three such tools.

2.1 Laboratory-scale test equipment

Figure 2 shows a photo of the developed laboratory scale test equipment (A=0.025 m^2 effective separator cross section). The air was supplied by a compressor in the laboratory. The pressure was first regulated by a dedicated pressure regulator valve (1). This static pressure plays a key role because the downstream fluidised bed and the technical air distribution system represent a given flow resistance and that determines how much energy is consumed, namely what air flow rate will be developed in the common operating point.

The air flow rate was measured indirectly by a Venturi tube (2) and a differential pressure meter (3). The lab-scale fluidised bed separator (4) had two parts, the bottom, and the top. The air distribution system was built into the bottom part. Many different systems were tested to reach stable fluidising conditions. The top part was made with transparent walls to allow us to observe flow disturbances.

2.2 Pilot-scale separator

Figure 3 shows two photographs of the pilot-scale aero-suspension dense media separator. The left -hand photo shows the side view and the right-hand photo shows the top view of the machine.

The machine is an aero-suspension dense media separator with an endless chain to discharge the separated products. A similar design was made by the China University of Mining and Technology in 1994 (Sahu, 2009; He et al., 2016). The so called CUMT separator was installed and operated in a coal mine of Qitaihe Coal Co. for dry coal upgrading. Figure 4 shows the schematic drawing of the chain system with 6 rollers. The 6 bearings of the chain routing rollers can be well seen on the left-hand side of Figure 3. The Venturi tube with a differential pressure meter and the air distribution head are also shown. Effective cross-sectional area of the bed is 0.146 m^2. The pilot-scale device was loaded with zirconium-oxide media, as shown on the right-hand side of Figure 3.

2.3 Industrial-size machine

Figure 4 shows the schematic drawing of the industrial scale aero-suspension dense media separator (the effec-

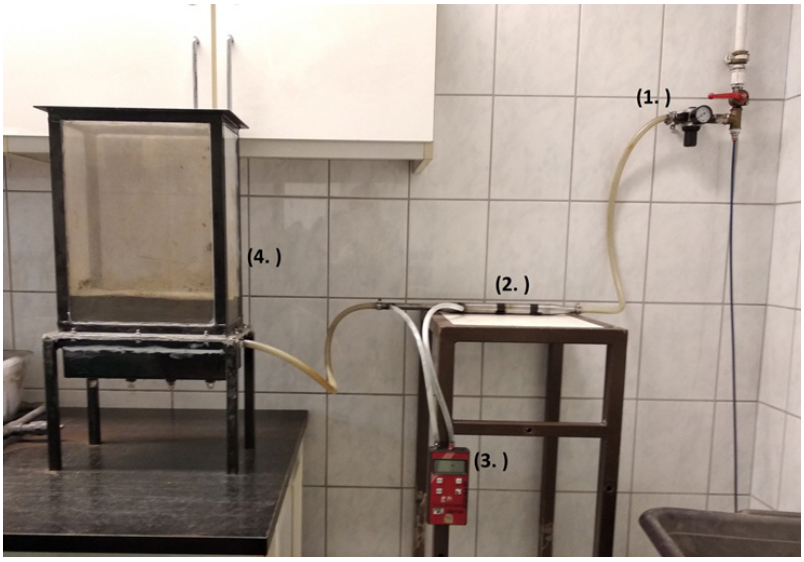

FIGURE 2: Laboratory scale test equipment (1 pressure regulator, 2 Venturi tube, 3 differential pressure meter, 4 laboratory model fluidised bed reactor).

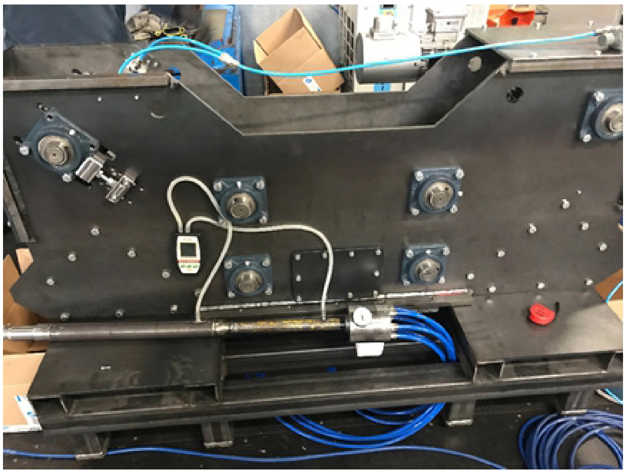

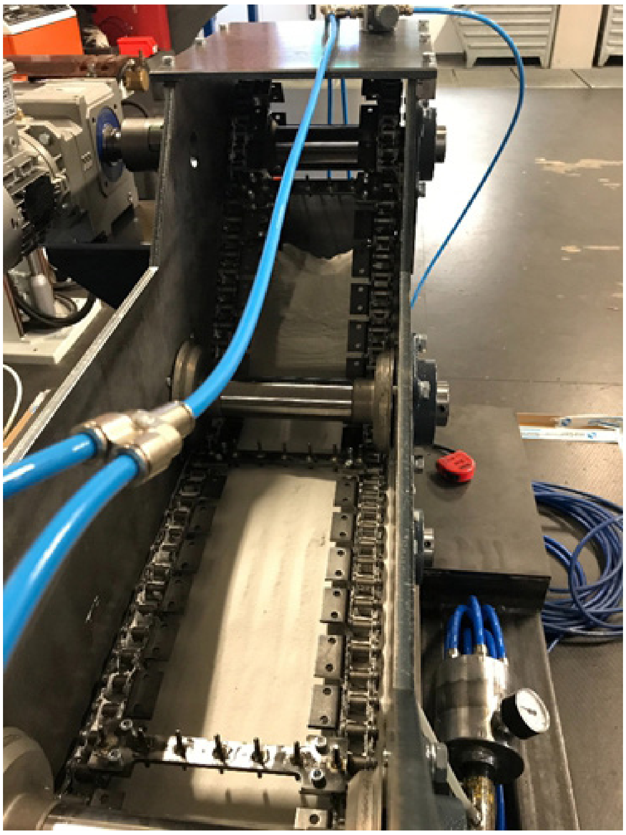

FIGURE 3: (Left) Side view of the pilot-scale aero-suspension dense media separator; (Right) Top view of the pilot-scale aero-suspension dense media separator.

tive cross-sectional area of the bed is 0.291 m^2). The mechanical engineering design of this machine was made by the Institute of Machine Tools and Mechatronics of the University of Miskolc. The machine has a massive steel frame. The frame is necessary to withstand the load because of the moving chain and comb elements of the discharge system in the fluidised bed. The discharge chain should work in non-fluidised separation medium as well. There are two endless chains at the front and back sides of the machine and cross-sectional combs are installed between them to discharge products. There are two toothed wheels and four non-toothed rollers. One toothed wheel is driven.

The centre part of the machine is charged with the bulk separation medium. The level of medium charge is higher than the level of the upper horizontal chain section, but it is lower than the product discharge points. The air is supplied by a compressor because the inlet pressure should be higher than 1 bar. There are built-in mechanical and air nozzle cleaning parts to clean the chains from the particles of the separation medium. The machine is modular; the width can be modified by changing the depth parts of it. Figure 8 shows a photo about the industrial scale machine.

2.4 Powder rheometer

The fluidisation behaviour of the different types of dense media was investigated in a Freeman Technology FT4 powder rheometer. During the measurements an air speed of up to 160 mm/s was used in a 25 mm measure-

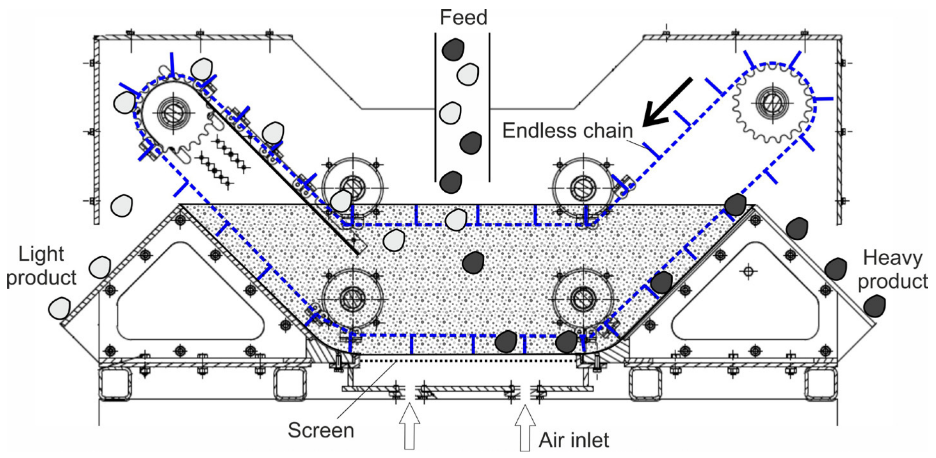

FIGURE 4: Schematic drawing and operational principal of the industrial-scale aero-suspension dense media separator.

ment cell to fluidise the material. These parameters were determined by preliminary tests. The total energy consumption for the rotation of a rotated paddle mixer (helix angle -5°) in the fluidised material was measured. The tip speed of the paddle was 80 mm/s.

2.5 Materials

Iron-oxide and zirconium-oxide powders were tested as working media during the development. The selection criterion of these materials was their high densities, because only with the application of high-density bed material can aero-suspension of suitable density be made. Different particle size fractions were made by manual laboratory sieving with a standard 200 mm laboratory sieve series. The size fractions were as follows in the case of iron powder: 0–100, 100–160, 160–200, 200–250, 250–315 and 315–400 µm.

The 160–400 µm iron powder size fraction was used for the laboratory scale fluidisation experiments and all others for the powder rheometer testing. The particle density of this fraction was measured many times in laboratory pycnometers; the average particle density was 6820 kg/m^3. The bulk density was measured by a volume calibrated glass cylinder; the average bulk density was 3085 kg/m^3. The porosity of the loosened bulk state iron powder fraction was ε_{mf}=0.548 (volume of air/volume of bulk). The mean shape factor of this used iron powder size fraction was determined by an optical microscope and image analysis (Φ=1.9; Figure 5).

Another material, zirconium-oxide, was also used for the laboratory-, pilot- and industrial- scale tests. The particle density of the 200–300 µm size fraction was 6060 kg/m^3 and the loosened bulk density was 3600 kg/m^3. The particle shape of zirconium-oxide can be considered spherical, according to image analysis (Φ=1; Figure 6).

The firm Inter-metal Ltd. collects mixed metal scrap from the area of Pest County, Hungary. The bigger metal pieces are cut by a guillotine shear as pre-shredding. Magnetisable particles are separated by a magnetic separator and fine particles are classified by sieving. The oversize product (30–100 mm) of the sieve goes into an eddy-current separator and its products are the useful conductive and the non-conductive contamination waste streams. The conductive product typically contains mainly aluminium and some copper. Without the aluminium–copper separation the value of this recycled metal is rather limited and this is the current challenge for the company. Samples were taken from the conductive product and one sample is shown on the left-hand side of Figure 9, used for the pilot-scale experiment described in Section 3.

3. RESULTS AND DISCUSSION

To understand the behaviour of the separation medium on the separation, fluidisation experiments were performed in a powder rheometer with iron powder and zirconia. The iron powder was divided into narrow particle size fractions and the measurements were performed with the size fractions given in Section 2.5. In the case of zirconia, balls with a nearly perfect spherical shape and very low surface roughness were used. Figure 7 shows the results of the fluidisation tests, where the total energy consumption to rotate a rotated paddle mixer with the same speed and path length in the fluidised material is presented. This total energy requirement was used to represent the effect of the air speed applied for the fluidisation of the material, and to evaluate the effect of the particle size and media type on the fluidisation of the media. For the 0–100, 100–160 and 160–200 µm fractions of the iron powder, as well as in the case of the zirconia balls (200–300 µm), the liquid-like behavioural state was reached, since the energy required to rotate the mixer stabilised as a function of the air velocity. For the coarser iron powder fractions, the air velocity was proved to be too low to achieve liquid-like behaviour. Mixing the iron powder without air velocity required much more energy than was required for zirconia balls, which can be explained by the spherical shape and smooth surface of the zirconia balls. For the different fractions of the iron powder, 160–200 mJ of total energy was measured without the use of air, while for the zirconia balls it was only 30–40 mJ.

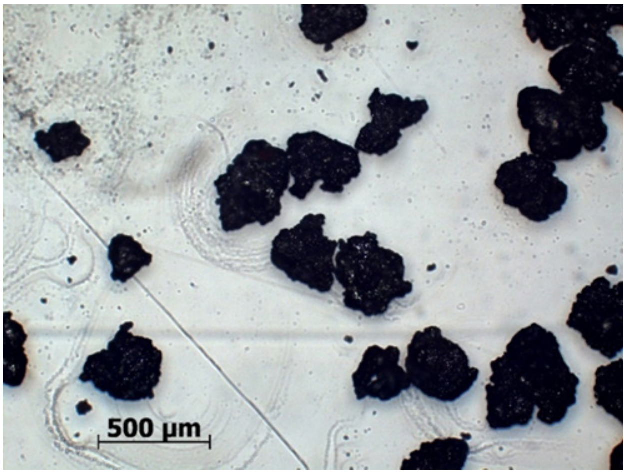

FIGURE 5: Particle shape of iron powder taken by an optical microscope.

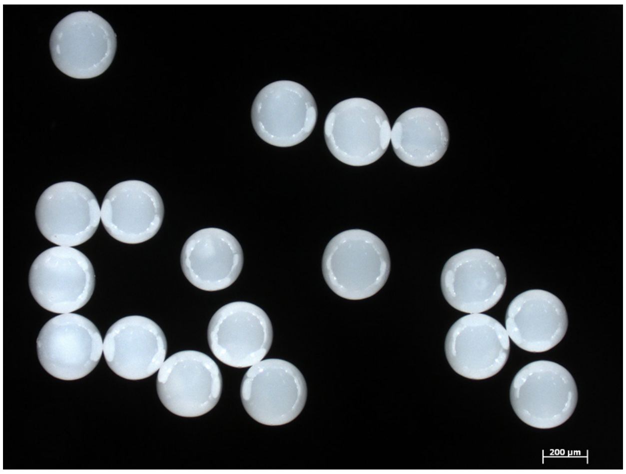

FIGURE 6: Particle shape of zirconia taken by an optical microscope.

This is of great importance in the design of the mechanical material discharger of the separator, as a much lower power drive chain may be required using the zirconia balls. As a result of the fluidisation, in the case of iron powder, the energy required to rotate the mixer was reduced by 30–50 times compared to the initial state.

If we examine the necessary air velocity for the liquid-like behaviour for each fraction, we can see that with the maximum particle size of the fraction, the required air velocity increases linearly in the case of iron powder. In the case of the zirconia balls, liquid-like behaviour was achieved at an air velocity lower than that of the iron powder compared to its particle size. Based on the performed tests, the separation medium should be as narrowly distributed in size as possible to be able to accurately adjust the air velocity required to reach the fluid state. The separation medium should have the smallest but still suitable particle size, because in this case a significantly lower air velocity is necessary for the fluidisation, which determines the required air flow. A medium with spherical particle shape seems to be more advantageous, as much less energy will be required to operate the separator.

Preliminary experimental series were carried out with the lab-scale test rig shown in Figure 2. Various quantities (m) of 160–400 μm iron powder were placed in the equipment and the non-fluidised height (H_{nf}) of the charge was measured first. Then the spring valve of the pressure regulator was gradually opened to a given point to set the regulated pressure after the regulator. Fluidisation conditions of the charge were visually observed. If the regulated pressure was too low, and therefore the air flow was too low, insufficient fluidisation took place. Increasing the pressure firstly resulted in good fluidisation conditions, while further increase led to increasingly high dust formation above the charged bed. The condition of the fluidised bed was manually checked by some aluminium and copper scrap particles hanging on wires. The surface of the fluidised bed looked like boiling water; many times, bubbles were randomly released. Figure 8 shows the industrial machine filled with zirconium-oxide charge and a bubble is clearly visible. Even though – on the surface – bubbling and dusting phenomena were not constant, the average height of this "bubbling zone" was also measured. A level increase of the charge in the reactor was not observable, only a bubbling zone developed above the material bed. Table 1 shows the measured results.

Results shown in Table 1 highlighted a design problem with the lab-scale test device, namely that the air velocity was too high in the air supply tubing, and therefore this pipe system was modified afterward. Pressure loss of the small tubing air supply was significant compared to that of the fluidised bed. Based on the results of the lab-scale tests the pilot-scale machine (Figure 3) was designed and built. Systematic fluidised bed fundamental and separation experiments were carried out. One of the aims of these tests was to determine the air supply requirements for the industrial size machine. The charge was filled into the 0.146 m^2 effective surface area pilot-scale machine at a non-fluidised height of 30 cm and the pressure regulator was set to 0.26; 0.38 and 0.4 bar-s. The measured air flow rates were 121; 148.7 and 159 m^3/h respectively. Although the set regulator pressure differences were relatively small, totally different fluidisation conditions were achieved: non-sufficient fluidisation for the smallest pressure, good fluidisation with slight air breakthrough for the medium and unacceptable air breakthrough for the highest was observed. For the air flow rate measurements a Venturi tube was used. The diameter of the smaller Venturi

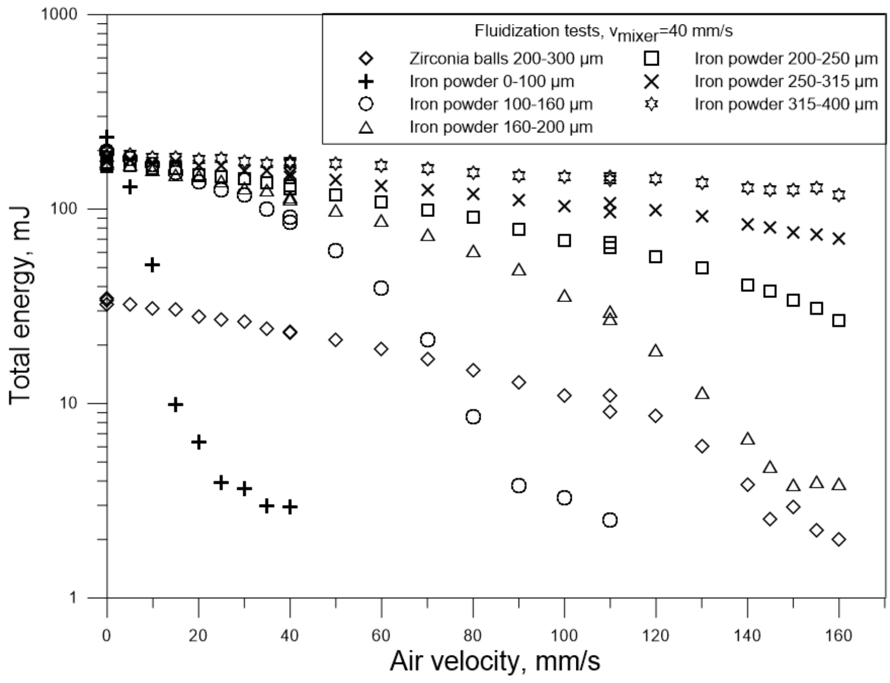

FIGURE 7: Fluidisation test results of the different media.

TABLE 1: Results of preliminary experiments carried out with the lab-scale test rig.

No. 1.	**mass of charge, m = 8 kg; non-fluidised height, H_{nf} = 11 cm;**				
Regulated pressure after the regulator [bar]	1	1.5	2	2.5	3
Height of bubbling zone [cm]	2	3	4	5	6
Air velocity in the 21 mm supply tube [m/s]	87.6	101.6	110.2	119.7	127.5
Condition	Not working	Not working	Not working	Not working	Not working
No. 2.	**mass of charge, m = 12 kg; non-fluidised height, H_{nf} = 15 cm;**				
Regulated pressure after the regulator [bar]	1	**1.5**	2	2.5	3
Height of bubbling zone [cm]	0	**3**	4	6.5	8.5
Air velocity in the 21 mm supply tube [m/s]	92.4	**105.4**	114.9	123.9	129.5
Condition	Not working	**Good**	High dust	High dust	High dust
No. 3.	**mass of charge, m = 16 kg; non-fluidised height, H_{nf} = 16.5 cm;**				
Regulated pressure after the regulator [bar]	1	**1.5**	2	2.5	3
Height of bubbling zone [cm]	0	**2**	4	6	8
Air velocity in the 21 mm supply tube [m/s]	87.6	**101.4**	111.3	120.5	134.7
Condition	Not working	**Good**	High dust	High dust	High dust

pipe section was 0.027 m and that of the bigger pipe section was 0.04 m. When good fluidisation was taking place the pressure loss on the Venturi tube was 1700 Pa, which corresponds to 148.7 m^3/h air flow rate and 1021 m^3/m^2h specific air need for the pilot-scale separator. On the basis of the results of the pilot-scale tests the industrial machine (Figure 8) was designed and built. Systematic fluidised bed separation experiments were carried out.

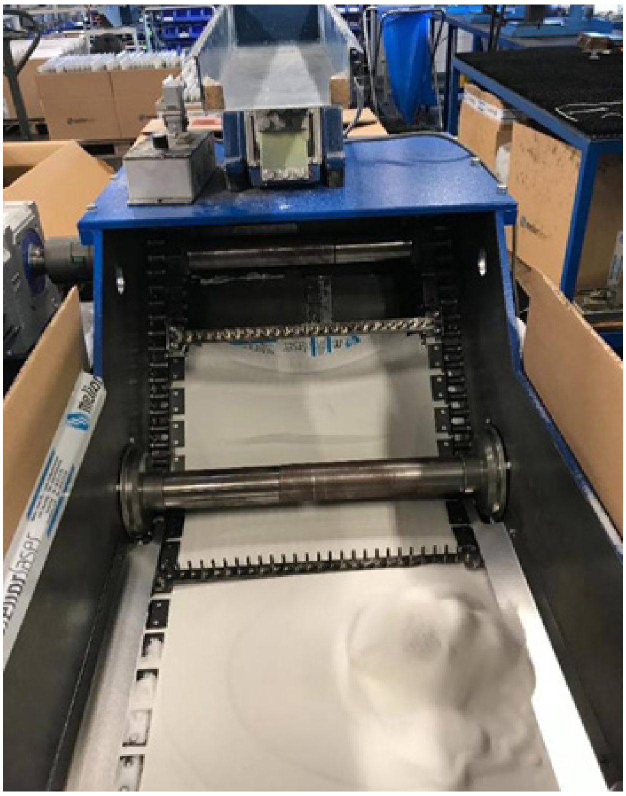

FIGURE 8: Photograph of the industrial-size aero-suspension separator.

Results of one test are shown here just as an example (Figure 9 left and right). Five kg of material was evenly fed to the equipment by a vibrated feeder for 60 seconds (Figure 9 left). Mass flow rate of feed was m_F = 300 kg/h. The copper-aluminium scrap sample is shown on the right-hand side of Figure 8. Mass yield of the Al product was g_{Al} = 81.25% and e_{Al} = 84.23% of the Al and e_{Cu} = 0% of the Cu in the feed was recovered to the Al product. Mass yield of the Cu product was g_{Cu} = 18.75% and e_{Al} = 15.77% of the Al and e_{Cu} = 100.0% of the Cu in the feed was recovered to the Cu product. 270 g of aluminium remained in the equipment. However, if the machine operates continuously, this remaining material is also discharged from the equipment. The Al product was pure a_{Al} = 100% aluminium, but the Cu product was not clean, it contained some aluminium. These incorrectly separated Al particles were probably discharged to the Cu product in two different ways: (1) an Al particle was stuck to the combs, travelled through the fluidised bed by the chain and then fell out on the Cu side; or (2) on the Cu side a dead space (non-fluidised separation medium) was formed and an Al particle which was trapped in this volume was discharged on the Cu side. Flat aluminium particles are difficult for the combs to handle. At discharge, flat particles may slip back into the separation space under the teeth of the combs (this was the reason for the 270 g of residual aluminium). Certain crumpled aluminium particles stick to the teeth of the combs, even very tightly, and the combs can make several turns with them. By installing more than one comb, the combs would be subjected to a lower load, so the capacity would be increased. The different magnitude tests that were carried out are a good basis to improve process engineering design methods of aero-suspension dense media separation. Table 2 summarises the main technical parameters of the laboratory, pilot and industrial scale machines and experiments.

The theoretical minimum differential pressure (Δp) that can provide enough hydrodynamic force to lift the particles

FIGURE 9: (Left) Feed of pilot experiment (30–100 mm copper-aluminium scrap); (Right) Products of pilot experiment (Al and Cu products).

of a given load of separation medium in a bed can be calculated from Eq. 2. Then the minimum fluidisation velocity (V_{mf}) can be calculated from the Ergun equation (Eq. 1). The quadratic Ergun equation was not solved analytically; instead, the positive solution of V_{mf} was iteratively calculated by Microsoft Excel. The earlier defined Reynolds number describing the air flow through the pores of the fluidised separation medium was calculated by Eq. 3. Results are shown in Table 3. The development and size upgrading of the different separators were based on the measured specific air need for sufficient fluidisation of a given separation medium charge. A theoretical specific air need value can also be calculated by Eq. 4. The minimum fluidisation velocity is the velocity of air through the pores, therefore, if this velocity is multiplied by a unit cross section (A_u) and divided by the porosity, the result is the specific air need (Q_s) for the given height of separation medium charge and machine.

$$Q_s = \frac{V_{mf} \cdot A_u}{\varepsilon_{mf}} \quad (4)$$

The height of the iron powder load in the laboratory separator is almost half that of the zirconium-oxide charge in the pilot-scale and industrial equipment, but the necessary minimum fluidisation velocity is much higher. This result

TABLE 2: Summary of different test data.

Test	Separation medium	Separator
LAB	iron powder d_p=280 μm; ρ_p=6820 kg/m^3; ε_{mf}=0.548; Φ=1.9	laboratory scale separator (Fig. 2) A=0.025 m^2; H_{mf}=0.165 m; m=16 kg
PILOT	zirconium-oxide d_p=250 μm; ρ_p=6060 kg/m^3; ε_{mf}=0.406; Φ=1	pilot scale separator (Fig. 3) A=0.146 m^2; H_{mf}=0.3 m; m=158 kg
IND	zirconium-oxide d_p=250 μm; ρ_p=6060 kg/m^3; ε_{mf}=0.406; Φ=1	industrial scale separator (Fig. 8) A=0.291 m^2; H_{mf}=0.3 m; m=315 kg

TABLE 3: Measured and calculated main technical parameters for laboratory-, pilot- and industrial-scale equipment.

	Calculated					Measured	
Test	H_{mf} [m]	V_{mf} [m/s]	Re_{mf} [-]	Δp [bar]	Q_s [m³/m²h]	p [bar]	Q_s [m³/m²h]
LAB	0.165	0.886	31.44	0.031	5823	1.5	5057
PILOT	0.3	0.148	2.47	0.106	1313	0.38	1021
IND	0.3	0.148	2.47	0.106	1313	0.38	1021

is in good correlation with the powder rheometer tests, indicating that the particle shape of iron powder is not spherical, and its surface is not smooth. The industrial size separator is a wider machine than the pilot-scale version; therefore, all of their calculated and measured specific data in Table 3 are identical. The difference is in the mass of the separation medium charge and in the separator surface. The calculated theoretical minimum differential pressure is significantly lower than the measured pressure after the regulator valve. In the case of the laboratory separator, it is much smaller. This indicates an initial insufficient machine design because the head pressure after the regulator valve supplies all the flow losses of the connecting pipes, the air distribution system and most importantly the drilled holes in the distribution pipe sections. Too small diameters of structural components of the laboratory separator were used. Although the necessary quantity and pressure of air were supplied for the fluidisation, the auxiliary losses were too high. The specific air need values measured and calculated (by Eq. 4) are very similar. This indicates that the Ergun equation can be used for the process engineering design of aero-suspension dense media separation. If the material properties of the separation medium are known, the air need for a given height separation medium load can be estimated by Eq. 4 using the Ergun minimum fluidisation velocity. The head pressure of the air supply system must be higher than the calculated minimum value. The calculation of the head loss of the air supply and distribution system can be determined by standard fluid dynamics calculations. This means that using the presented method, an aero-suspension dense media separator can be designed by just knowing the material features without any tests. This developed and validated process engineering design method of gas-solid fluidised bed separators can be used by both academia and industry.

4. CONCLUSIONS

A laboratory scale fluidised bed separator was built and charged with different granular materials to study fluidisation. A pressure regulator can be applied and by opening its spring valve up to a given point, a steady-state air flow rate can be set. If the air supply was low the charged bed was not fluidised. There was only a very narrow air flow rate range within which a good fluidised bed was formed. In this narrow range, the surface of the charged bed started to "boil", forming bubbles. Al particles floated and Cu particles settled in this good fluidised bed. If the air flow rate was further increased, bubbling increased and dust was released, and the operational conditions were no longer appropriate.

Different size fractions of iron powder and zirconium-oxide were tested in a powder rheometer. Mixing the iron powder without air fluidisation required much more energy compared to mixing zirconia balls, which can be explained by the spherical shape and smooth surface of the zirconia balls. The fluidised powder rheological tests resulted in much lower driving energy for the zirconia balls. As a general conclusion a narrower particle size distribution of the separation medium is better because fluidisation is easier and spherical shape and smooth surface are better because of the lower mixing (fluidisation) energy need. Based on the results of the lab-scale tests a pilot-scale and later an industrial scale machine (400 kg/h) were designed and built. Separation experiments were carried out with aluminium-copper scrap in the 30–100 mm particle size range. This is a limitation of the machine, because only this size range can be separated with this machine. The Al products were typically clean, but the Cu products contained some aluminium contamination. For the Cu product a secondary separation step might be necessary to produce pure copper. The Ergun model was used to calculate the minimum pressure difference and fluidisation air velocity for separation experiments with iron powder and zirconia at the scale of the laboratory, pilot and industrial-size equipment. It is concluded that the specific air need of a given type and height separation medium machine can be calculated by the Ergun model, because the measured and calculated values are in good agreement. The measured pressures after the air supply regulator valves were higher than the calculated Ergun minimum differential pressures because the air supply system covers the flow losses of the pipes, air distribution system and also the drilled holes of the distribution pipe sections. When the machine design is proper these auxiliary losses are low but cannot be zero.

In addition to the machine development, the developed process engineering design method on the basis of the newly introduced specific air need for a given height of separation medium charge parameter for gas-solid fluidised bed separators has the advantage, that – even without building the machine – the technical parameters can be calculated just on the basis of results of simple material testing.

AKNOWLEDGEMENTS

The project was supported by the Hungarian National Research, Development and Innovation Office from the NKFI Fund, "Creation of the first Hungarian dry dense media separation technology and prototype for the processing of mixed aluminium wastes and marketing the separated goods", project no.: KFI_16-1-2017-0324.

REFERENCES

Anam, A. C., & Ikhwan, N. (2020). Experimental study of particle separation using fluidised bed method. THERMOFLUID X: 10th International Conference on Thermofluids 2019. https://doi.org/10.1063/5.0020175

Anjaneyulu, P., & Khakhar, D. (1995). Rheology of a gas-fluidized bed. Powder Technology, 83(1), 29–34. https://doi.org/10.1016/0032-5910(94)02922-b

Basu, P. (2006) Combustion and gasification in fluidized beds. CRC Press.

Beeckmans, J. M., & Minh, T. (1977). Separation of mixed granular solids using the fluidized counter-current cascade principle. The Canadian Journal of Chemical Engineering, 55(5), 493–496. https://doi.org/10.1002/cjce.5450550501

Dévay, A. (2013). Fundaments of pharmaceutical technologies. Pécs University of Sciences. (in Hungarian)

Drzymala J. (2007). Mineral Processing, Foundations of theory and practice of minerallurgy. Wroclaw University of Technology.

Ergun, S. (1952). Fluid flow through packed columns. Chemical Engineering Progress 48, 9-94

Everett, J. W., & Peirce, J. (1990). The development of pulsed flow air classification theory and design for municipal solid waste processing. Resources, Conservation and Recycling, 4(3), 185–202. https://doi.org/10.1016/0921-3449(90)90001-k

Fan, X., & Zhou, C., (2021) Estimation of Bed Expansion and Separation Density of Gas–Solid Separation Fluidized Beds Using a Micron-Sized-Particle-Dense Medium. Separations 8(12), Article 242; https://doi.org/10.3390/separations8120242

Ghosh, T. (2013). Modeling of an air-based density separator. PhD. Thesis. University of Kentucky. (http://uknowledge.uky.edu/mng_etds/7)

Gibilaro, L. G. (2001). Fluidization dynamics. Butterworth-Heinemann.

He, J. Tan, M. Zhu, R. & Luo, Z. (2016) Dry beneficiation and cleaning of Chinese high-ash coarse coal utilizing a dense-medium gas-solid fluidized bed separator. Physicochemical Problems of Mineral Processing, 52(2) 662–675. https://doi.org/10.5277/ppmp160212

Hou, W., Man Li, R.Y., & Sittihai, T., (2022) Management Optimization of Electricity System with Sustainability Enhancement. Sustainability 14, Article 6650. https://doi.org/10.3390/su14116650

Krüger, B., Mrotzek, A., & Wirtz, S. (2014). Separation of harmful impurities from refuse derived fuels (RDF) by a fluidized bed. Waste Management, 34(2), 390–401. https://doi.org/10.1016/j.wasman.2013.10.021

Oshitani, J., Kajiwara, T., Kiyoshima, K., & Tanaka, Z. (2003). Separation of Automobile Shredder Residue by Gravity Separation Using a Gas-Solid Fluidized Bed. KONA Powder and Particle Journal, 21(0), 185–194. https://doi.org/10.14356/kona.2003021

Pillay, K., Mainza, A.N., Chetty, D., & Becker, M. (2022). Mineralogical Factors Affecting the Dense Medium Separation of Nickel Sulfide Ores. Minerals, 12(10), 1311; https://doi.org/10.3390/min12101311

Li, Q., Shi, S., & Zhang, Y (2017) Application and Development Fluidised-bed Separator. Multipurpose Utilization of Mineral Resources, 3, pp: 29-31, 37. https://doi.org/10.3969/j.issn.1000-6532.2017.03.004 (in Chinese)

Sahu, A. K., Biswal, S. K., & Parida, A. (2009). Development of Air Dense Medium Fluidized Bed Technology For Dry Beneficiation of Coal – A Review. International Journal of Coal Preparation and Utilization, 29(4), 216–241. https://doi.org/10.1080/19392690903113847

Sekito, T., Matsuto, T., & Tanaka, N. (2006). Application of a gas–solid fluidized bed separator for shredded municipal bulky solid waste separation. Waste Management, 26(12), 1422–1429. https://doi.org/10.1016/j.wasman.2005.10.015

Trung Thanh, B., & Anh Duc, L. (2020). Determination on Fluidization Velocity Types of the Continuous Refined Salt Fluidized Bed Drying. In I. Pala-Rosas (Ed.), Current drying processes. Intech. https://doi.org/10.5772/intechopen.92077

Yoshida, M., Nakatsukasa, S., Nanba, M., Gotoh, K., Zushi, T., Kubo, Y., & Oshitani, J. (2010). Decrease of Cl contents in waste plastics using a gas–solid fluidized bed separator. Advanced Powder Technology, 21(1), 69–74. https://doi.org/10.1016/j.apt.2009.11.002

Zhao, Y., & Wei, L. (2000). Rheology of gas–solid fluidized bed. Fuel Processing Technology, 68(2), 153–160. https://doi.org/10.1016/s0378-3820(00)00122-3

Zhou, C. Dong, L. Zhao, Y., & Fan, X. (2019). Studies on Bed Density in a Gas-Vibro Fluidized Bed for Coal Cleaning. ACS Omega, 4(7),12817–12826. https://doi.org/10.1021/acsomega.9b01892

Zhumadillayeva, A., Orazbayev, M., Santeyeva, S., Dyussekeyev, K., Yi Man Li, R., Crabbe, J. C. (2020) Models for Oil Refinery Waste Management Using Determined and Fuzzy Conditions. Information, 11(6), 299; https://doi.org/10.3390/info11060299